SUPPLEMENTAL FIGURES

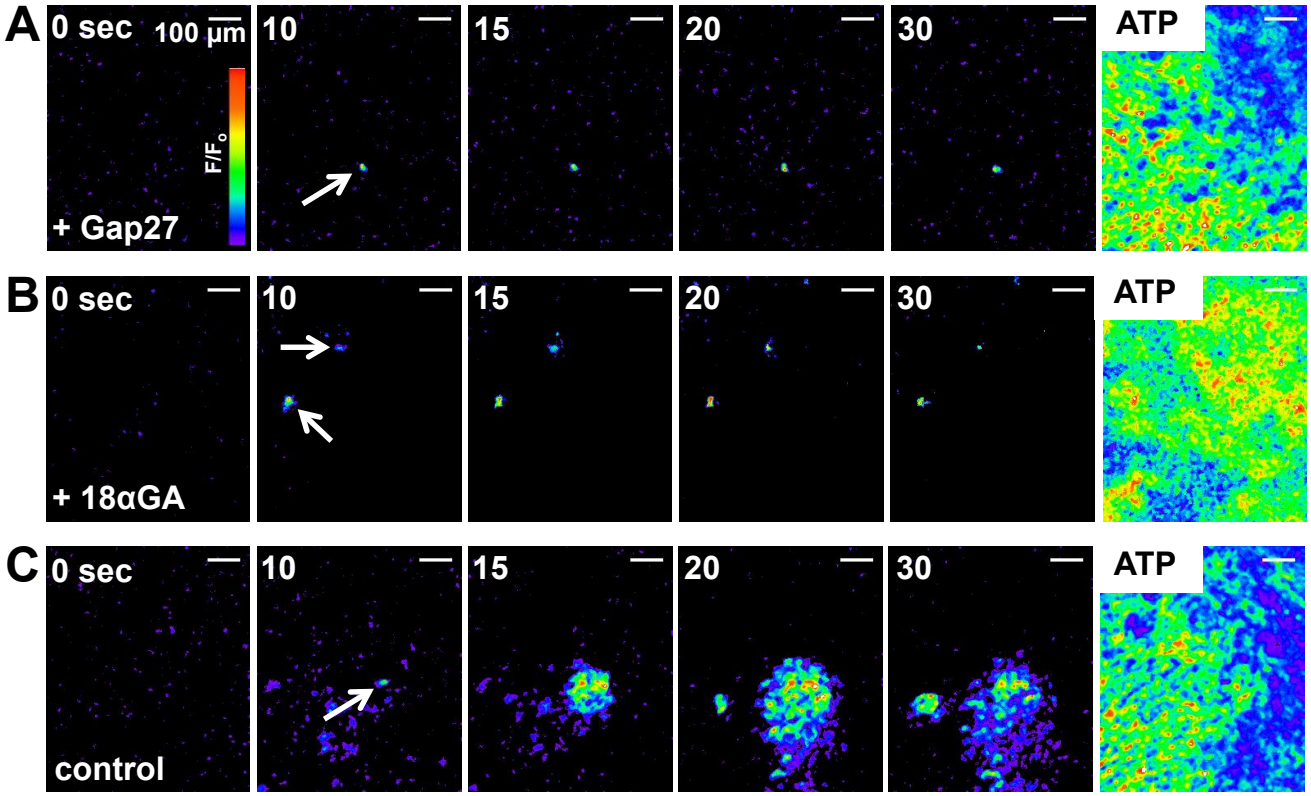

Supplemental Figure 1
Propagation of the denatonium-induced calcium signal is sensitive to gap junction inhibitors Gap27 and 18α-glycyrrhetinic acid (18α-GA). ALI cultures were pre-incubated with PBS (control), 300 µM Gap27 (1 hr), or 100 µM 18α-GA (30 min). First panel indicates time immediately before denatonium stimulation (time 0) followed by 10, 15, 20, and 30 seconds after denatonium stimulation. Last panel shows the same field upon subsequent stimulation with 10 µM ATP. (**A**) In the presence of Gap27, denatonium stimulation resulted in calcium responses from single solitary cells. Experiment shown is representative of 4 independent experiments using cultures from 4 different patients. (**B**) 18α-GA also resulted in denatonium-activated calcium responses that did not appear to propagate to surrounding cells in cultures. Image representative of 4 independent experiments from the same 4 patients. (**C**) Control experiments (PBS alone) were performed using cultures from the same 4 patients used in A-B. In the absence of gap junction inhibitors, denatonium-stimulated calcium responses appeared to originate at single cells but rapidly spread to the surrounding cells.

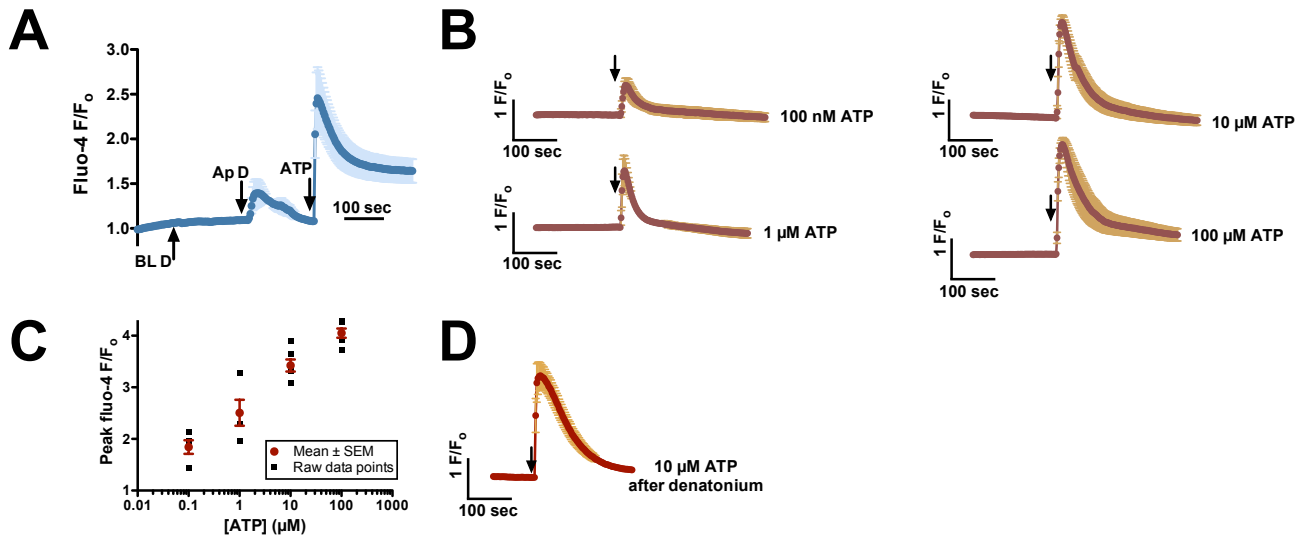

Supplemental Figure 2
Evaluation of the polarity of the denatonium-induced calcium response and effects on purineric-induced responses. (**A**) Polarity of the ALI response to denatonium benzoate stimulation. Denatonium benzoate (10 mM) induced a calcium response when applied apically (Ap D), but not when applied basolaterally (BL D). Response to apical application of the puringeric agonist ATP (10 µM) is shown as a control. Trace shows 1 representative experiment (mean ± SEM of 6 cells) out of 6 experiments using ALIs from 3 patients. (**B-D**) Denatonium stimulation did not inhibit the subsequent calcium response to ATP, confirming cell viability. Average traces (**B**; mean ± SEM; n = 3-5 experiments each) and dose response plot (**C**) of naïve (no prior denatonium) ALI cultures' responses to ATP stimulation at 4 concentrations. ATP response was not affected after stimulation with 10 mM denatonium benzoate (**D;** n = 6 ALIs from 3 patients).

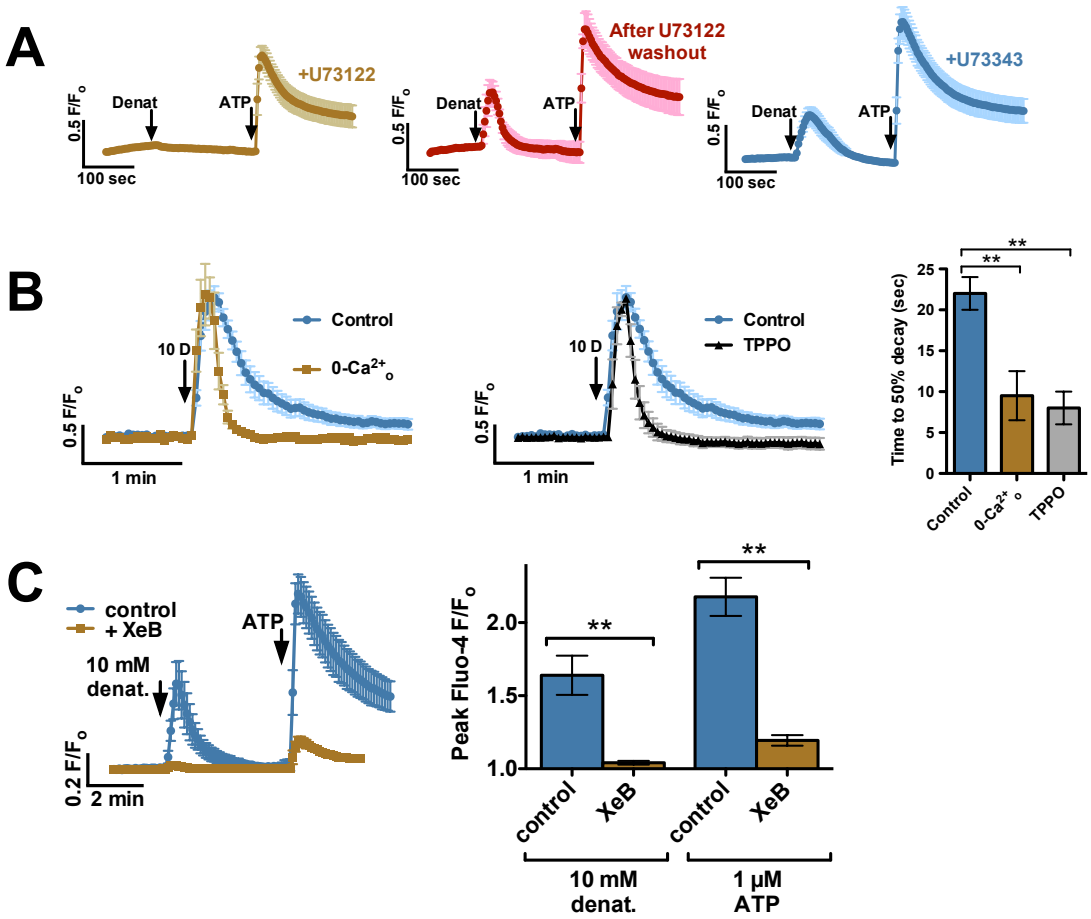

Supplemental Figure 3
Pharmacological evaluation of the denatonium-induced calcium response. (**A**) Denatonium benzoate-induced calcium signaling is inhibited by inhibition of PLCβ2, an important component of taste signaling. The PLCβ2 inhibitor U73122 (10 µM; applied apically) inhibited denatonium-induced calcium signaling, confirming that this response is likely due to G-protein—coupled receptor activation (left panel). Effects of U73122 were reversed after washout (middle panel). The inactive analogue of U73122, U73343, did not inhibit denatonium-induced calcium signaling (right panel). Traces show mean ± SEM of 5 experiments each. (**B**) The duration, but not the magnitude of denatonium-induced calcium signaling is inhibited by removal of extracellular calcium or inhibition of the TRPM5 ion channel. When extracellular calcium was chelated (0-Ca^{2+}_o/1 mM EGTA), the duration of the denatonium induced calcium response was shortened despite no effect on the peak calcium response (left panel). Experiments were performed in the presence of carbenoxolone (150 µM) to block gap junction communication so as to record only the denatonium-responsive cells themselves. These data suggest that the initial calcium signal reflects release of calcium from intracellular stores while calcium influx is required for extending the duration of the calcium response. The TRMP5 inhibitor TPPO (100 µM) (1) also inhibited the duration of the calcium response similarly to removal of extracellular calcium (middle panel). The signal transduction cascade described in type II cells of the tongue places TRPM5 downstream of calcium release (2); calcium activates TRPM5, which is permeable to Na^+ and causes depolarization that could activate calcium influx through voltage gated channels. This result supports a role for extracellular calcium in the duration of the denatonium response in sinonasal epithelial cells but also suggests this response occurs through the taste signaling pathway. Right panel shows a bar graph showing time from peak F/F_o to 50% return to baseline under control (n = 14 cells from 5 experiments), 0-Ca^{2+}_o (n = 7 cells from 3 experiments), and TPPO (n = 6 cells from 3 experiments) conditions; asterisks indicate significance determined by 1-way ANOVA with Dunnett's post test. (**C**) The IP3R inhibitor xestospongin B (XeB; 10 µM, 30 min pre-incubation) reduced the magnitude of both denatonium- and ATP-induced calcium responses (n = 5-6 experiments each). Asterisks in bar graph represent significance determined by 1-way ANOVA with Bonferroni post test. For all graphs, * = P <0.05, ** = P <0.01.

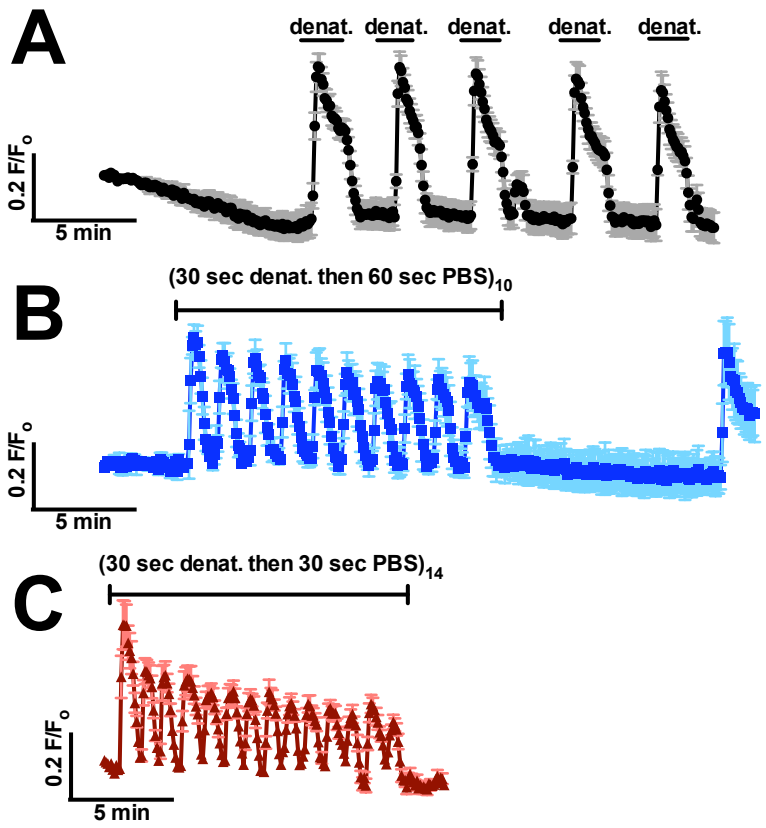

Supplemental Figure 4
Repeated stimulation with a T2R agonist resulted in minimal tachyphylaxis or desensitization.
(**A**) We noted that repeated stimulation with denatonium resulted in minimal tachyphylaxis, suggesting that SCC calcium signaling pathways recover quickly. The apical membrane was perfused with PBS solution or PBS + denatonium. Image shown is representative of 3 experiments. (**B**) An experimental protocol was followed where cultures were stimulated with 10 mM denatonium for 30 sec followed by 60 sec washout with PBS for 10 cycles. No significant tachyphylaxis was observed. Image shown is representative of 3 experiments. (**C**) Some tachyphylaxis was observed during a protocol where cells were stimulated for 30 sec with denatonium followed by only 30 sec washout with PBS. However, a signal was still observed after 14 cycles. Image representative of 3 experiments.

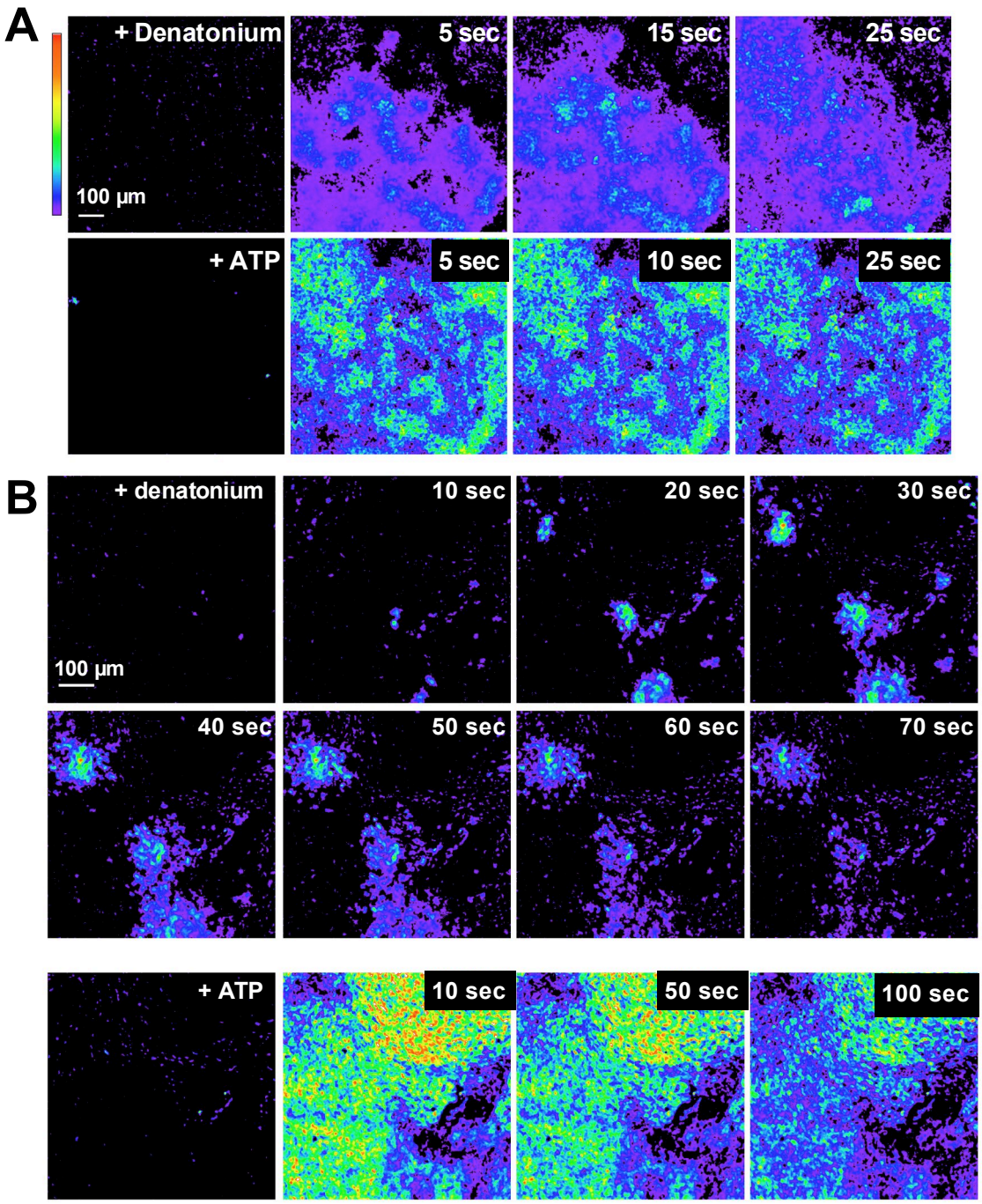

Supplemental Figure 5
Responses to denatonium benzoate in human bronchial epithelial (HBE) cultures and sinonasal explants. (**A**) Denatonium induces a more global calcium response in HBE cells. Images shown are representative of 10 different cultures stimulated with 10 mM denatonium benzoate. Image is representative of 18 ALIs from 5 patients. (**B**) Denatonium stimulation results in localized calcium signaling in human sinonasal tissue explants. Images shown are representative of 6 experiments performed using tissue from 3 different patients. Tissue was loaded with Fluo-4-AM for 30 min in HBSS, then washed thoroughly with PBS and gently clamped upside down on an inverted confocal microscope (cilia facing the objective) using an open bath RC-22 chamber (Warner Instruments, Hamden, CT). Denatonium was added to the bath from a 2x stock solution to a final concentration of 10 mM. ATP was added to the bath from a 10x stock solution to a final concentration of 100 µM. Calcium signals in response to denatonium (but not ATP) appeared to originate from discreet cell(s) distributed throughout the epithelium. Representative of 12 experiments from tissue samples from 3 patients.

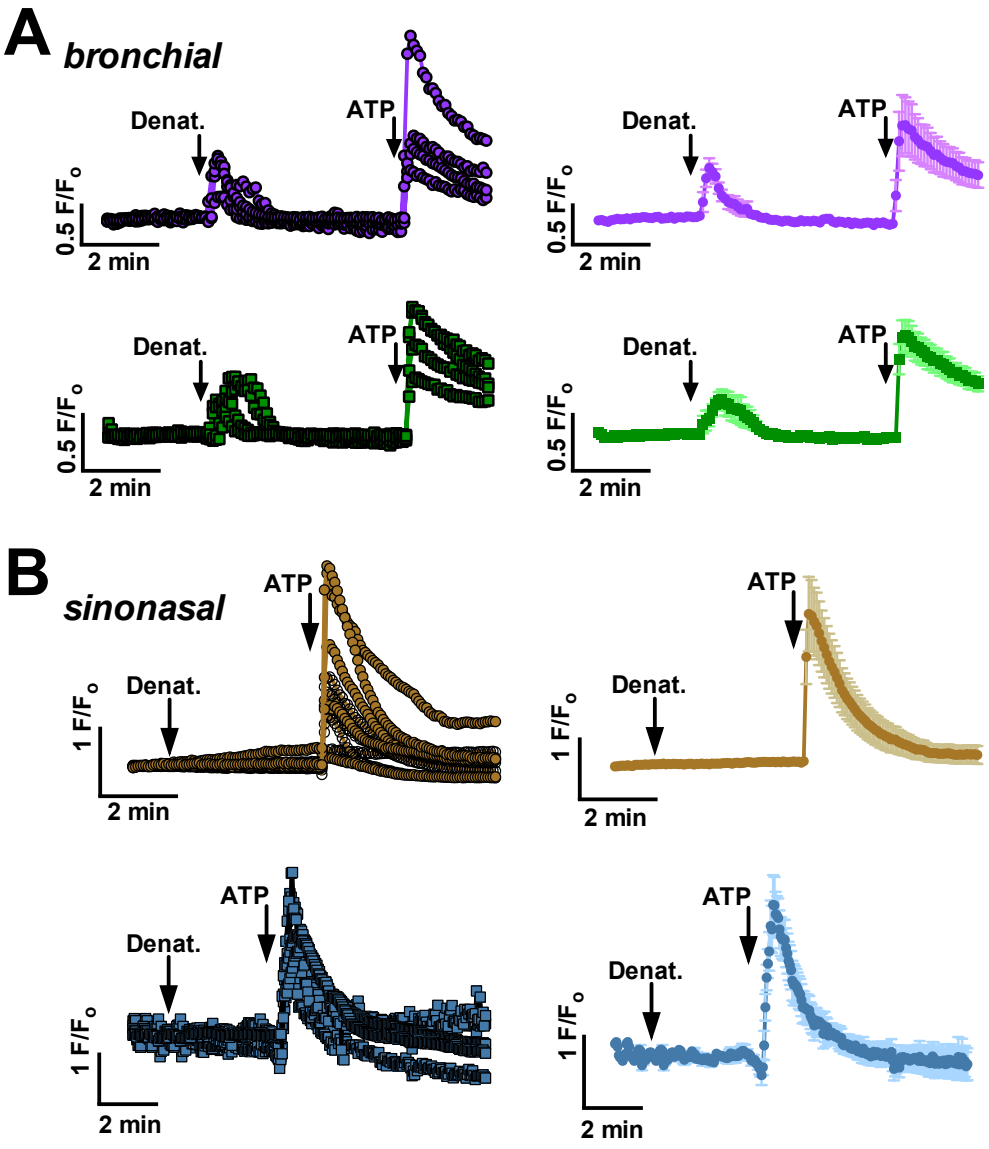

Supplemental Figure 6
Responses to denatonium benzoate in freshly dissociated sinonasal ciliated epithelial cells and dissociated human bronchial epithelial (HBE) cells. (**A**) Dissociated ciliated HBE cells (ciliation verified by observation under differential interference contrast) were isolated by gentle protease digestion. Ciliated cells exhibited intracellular calcium responses to both 10 mM denatonium benzoate and 100 μM ATP. Left graphs show each experiment raw data trace and right graphs show the respective mean trace ± sem. Top and bottom traces show results from 2 separate patients (n = 4 cells from each). (**B**) No responses were observed when acutely dissociated sinonasal ciliated epithelial cells were stimulated with 10 mM denatonium benzoate. Two separate patients (8 cells each) were observed and shown. Left graphs show each experiment raw data trace and right graphs show the respective mean trace ± sem. We previously observed that sinonasal ciliated epithelial cells directly respond to T2R38 agonists, but these data suggest that sinonasal ciliated epithelial cells do not express denatonium-sensitive T2Rs.

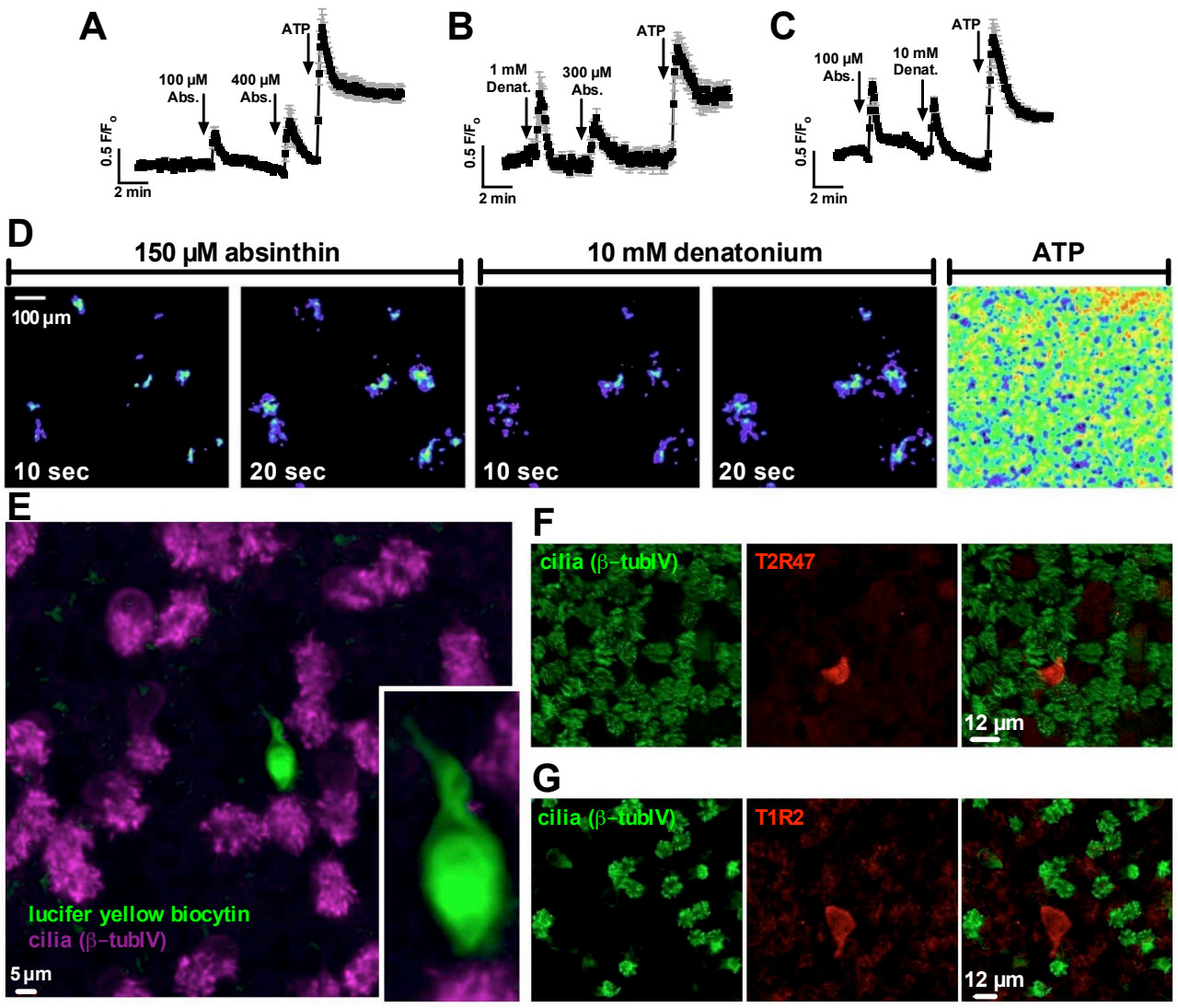

Supplemental Figure 7
The T2R receptor agonist absinthin activates calcium signals likely originating from the same cells as denatonium-stimulated calcium signals. (**A**) Representative average trace (± SEM) from one experiment (25 cells) responding to increasing concentrations of absinthin (3). (**B**) Representative average trace from one experiment (23 cells) showing that stimulation with absinthin after a low concentration of denatonium resulted in calcium signals in the same cells. (**C**) Representative average trace from one experiment (~26 cells) showing that stimulation with denatonium after a low concentration of absinthin resulted in calcium signals in the same cells. (**D**) Representative images (of 9 experiments) of an experiment showing sequential stimulation of absinthin, denatonium, and ATP. Patterns of absinthin-responding and denatnoium-responding cells were very similar. (**E**) Morphologic characterization of the denatonium responsive cell type was accomplished under live cell imaging with cells loaded with fluo-4 and treated with carbenoxolone. Following application of denatonium benzoate to the apical surface of the culture the responding cell was identified and impaled with a sharp electrode and lucifer yellow biocytin was injected into the cell using a microionophoresis current generator (Warner Instruments, Hamden, CT). The culture was then fixed and immunostained for type IV β-tubulin (a marker of respiratory cilia) demonstrating that the responding cell type is non-ciliated. (**F**) A similar non-ciliated unipolar morphology was observed when immunofluorescence was performed using antibodies directed against the denatonium- / absinthin-responsive T2R47 (4). (**G**) Immunofluorescence for the T1R2 subunit of the sweet receptor also revealed staining of solitary, non-cilaited cells. Images in (**F** and **G**) representative of staining observed in ALIs from at least 3 patients.

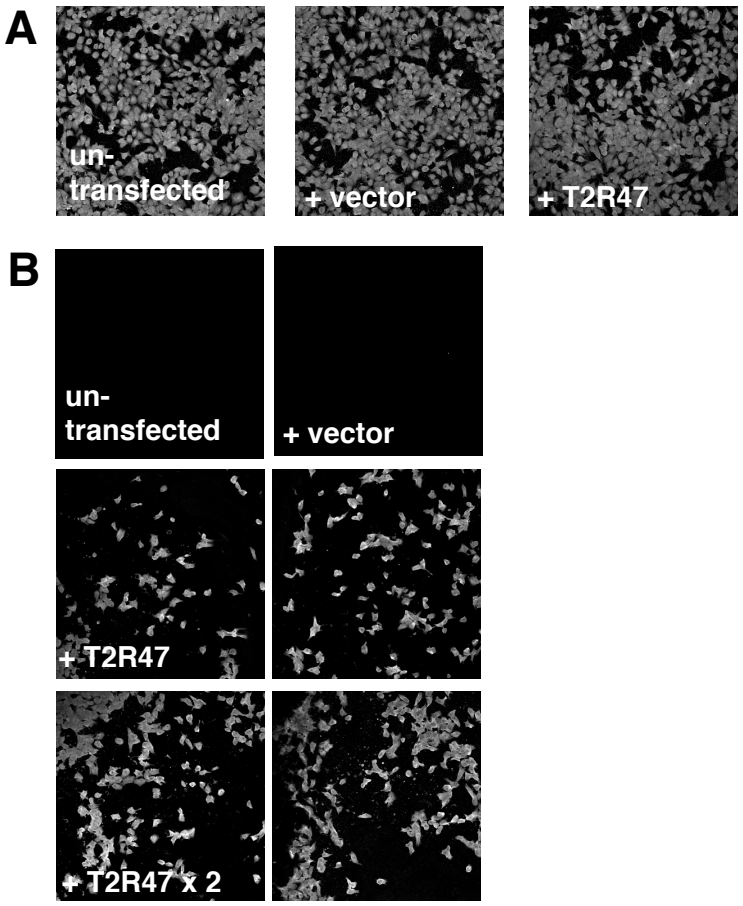

Supplemental Figure 8
T2R47 antibody immunofluorescence validation. HEK293 cells (as described previously [11]) were grown to ~80% confluence and transfected with empty vector (pcDNA3.1) or pcDNA3.1 containing human T2R47 approximately 24 hrs prior to fixation and immunofluorescent staining. (**A**) IP_3 receptor staining was similar among untransfected, vector only, and T2R47-transfected cells. (**B**) T2R47 immunofluroescence was only observed in transfected cells.

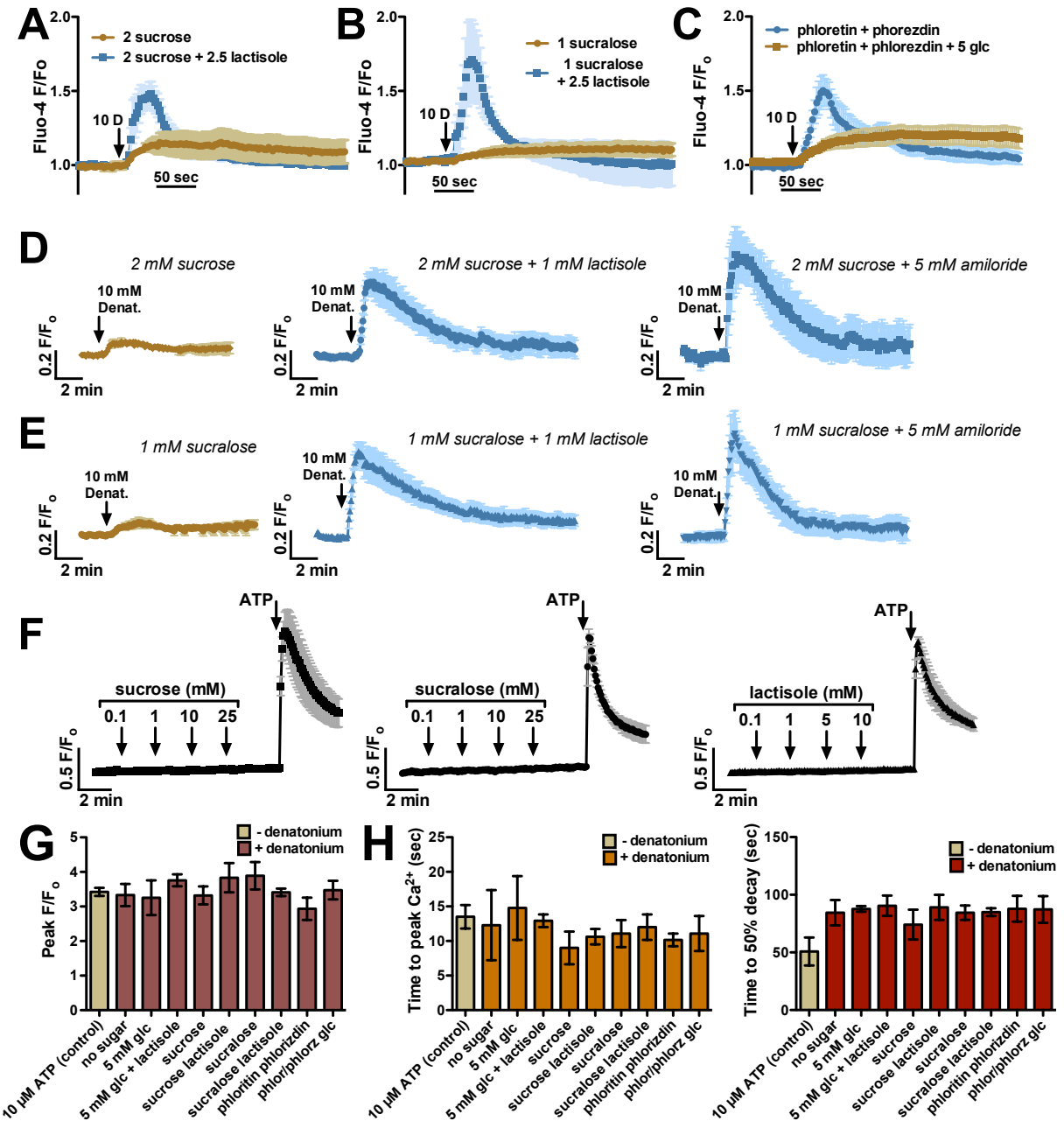

Supplemental Figure 9

The sweet agonists sucrose and sucralose inhibit the denatonium-induced calcium response in sinonasal ALI cultures via a mechanism likely involving the T1R2/3 sweet receptor. (**A-C**) Average traces (5-7 experiments each) showing inhibition of denatonium benzoate (10 mM)-induced calcium signaling by 2 mM sucrose (**A**) and 1 mM sucralose (**B**); inhibition was reversed by 2.5 mM lactisole. (**C**) The glucose transport inhibitors phloretin and phlorezin (100 µM each) did not prevent glucose-mediated inhibition of the denatonium induced calcium signal. (**D,E**) Sucrose and sucralose inhibition was also reversed by the sweet receptor antagonist, amiloride as well as lactisole. Traces are mean ± SEM from 4 cultures from 4 patients each. (**F**) High concentrations of sucrose, sucralose, or lactisole had no effects on *de novo* calcium signaling or ATP-induced calcium signaling. Traces are mean ± SEM of 4 cultures from 4 patients each. (**G-I**) Sweet receptor agonists had no effect on the magnitude (peak) or kinetics (time to peak or time to 50% decay) of global ATP-induced calcium signaling. Control bar ("- denatonium") shows response in naïve cultures (no prior denatonium stimulation; n = 7). Other bars ("+ denatonium") show responses in cultures after prior stimulation with 10 mM denatonium (n = 3 – 7 each). No significant differences observed via 1-way ANOVA.

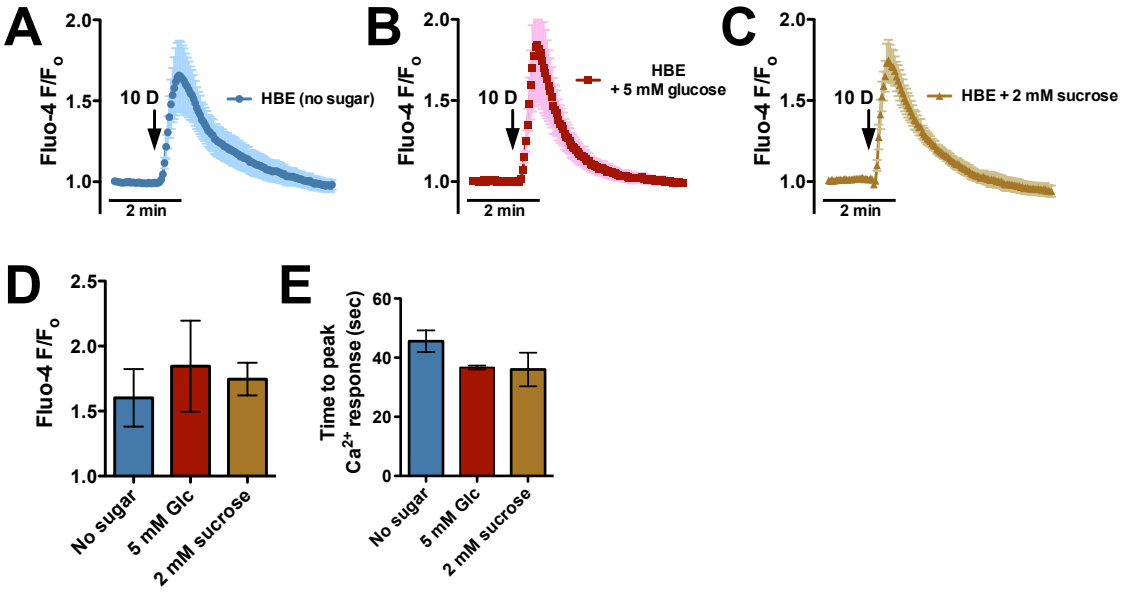

Supplemental Figure 10
Denatonium-induced calcium responses in human bronchial epithelial (HBE) cells were not inhibited by the T1R2/3 receptor agonists glucose or sucrose. (**A-C**) Average traces (5-7 experiments each using ALIs from 2-3 patients) of HBE cell calcium response to 10 mM denatonium benzoate in the absence of sugar (**A**) or in the presence of 5 mM glucose (**B**) or 2 mM sucrose (**C**). (**D**) Graph of peak calcium response from (**A-C**). (**E**) Graph of time to peak calcium response from (**A-C**). No significant differences were detected in (**D** and **E**) via 1-way ANOVA.

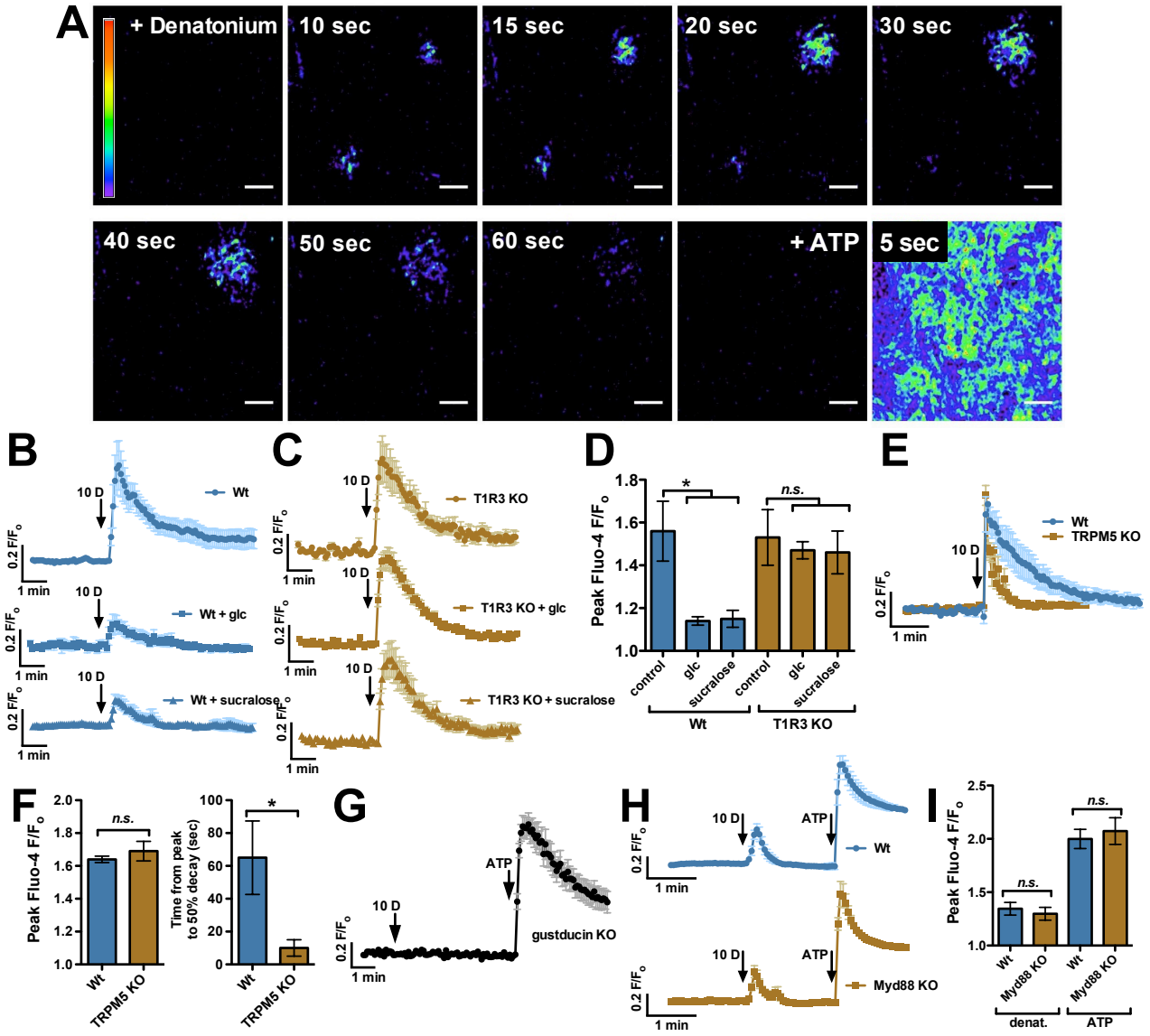

Supplemental Figure 11
In mouse nasal septal ALI cultures, denatonium activates localized calcium signaling that is inhibited by sweet receptor activation and involves TRPM5 and gustducin but not TLR signaling. (**A**) Representative F/F$_o$ image showing calcium response to 10 mM denatonium benzoate and 10 μM ATP. (**B** and **C**) Average traces (7-12 cultures from 4-6 mice each) showing response to 10 mM denatonium benzoate in Wt and T1R3 knockout (KO) cultures (5) in the presence of no apical sugar (control), 1.5 mM glucose, or 1 mM sucralose, an artificial sweetener that is a T1R2/3 receptor agonist. (**D**) Peak calcium responses from (**B** and **C**), showing that glucose and sucralose inhibited denatonium-induced calcium responses in Wt but not T1R3 KO mice. Asterisks denote significance between indicated groups determined by 1-way ANOVA with Bonferroni post test. (**E**) Average traces (5-7 cultures each from 3 mice) from Wt and TRPM5 KO (6) mouse nasal septal ALIs showing calcium responses to 10 mM denatonium benzoate. Experiments were performed in the presence of carbenoxolone to isolate single responding cells (n = 5 each). (**F**) In TRPM5 KO mice, the peak calcium response to denatonium was unaffected (left graph; no significant difference via Student's *t*-test), but the duration of denatonium-induced calcium responses was shortened (right graph; asterisk denotes significance determined by Student's *t*-test), similar to results in human cultures using the TRPM5 inhibitor TPPO (**Supplemental Fig. 2**) (**G**) Average trace (12 cultures from 4 mice) showing the response to 10 mM denatonium benzoate in cultures from alpha-gustducin KO mice (7). No responses were observed to denatonium despite robust responses to the purinergic agonist ATP. (**H**) As a control, the responses to denatonium were intact in Myd88 KO mice (n = 6 ALIs from 3 mice each for Wt and Myd88 KO), suggesting that the response is independent of TLR signaling. (**I**) Bar graph of peak responses from (**H**). There was no significant difference between indicated groups determined by either Student's t-test or 1-way ANOVA. Together, these data suggest that the denatonium-induced calcium response is similar in mouse and human ALI cultures and involves the taste signaling pathway. For all figures, * = P <0.05, ** = P <0.01, and *n.s.* = no statistical significance.

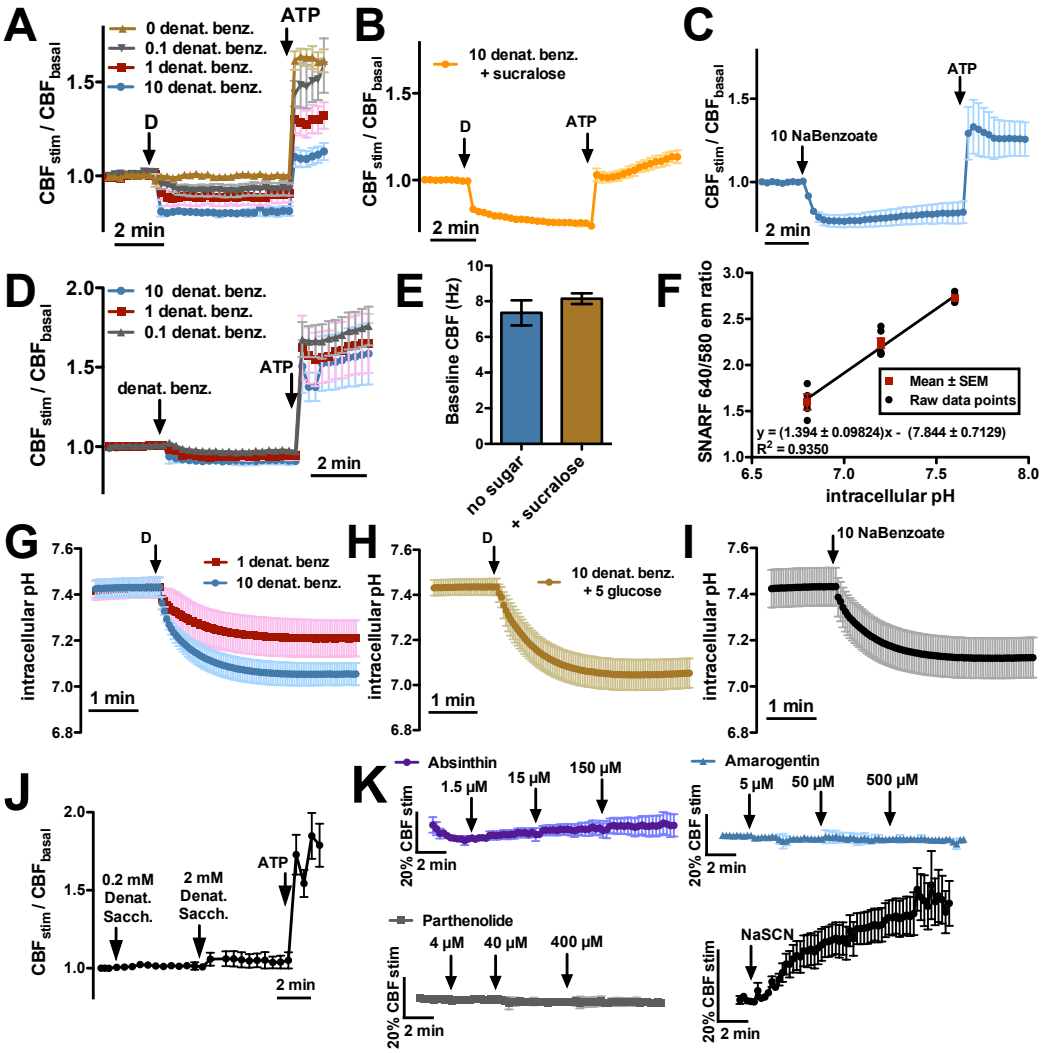

Supplemental Figure 12

Denatonium and absinthin do not elevate ciliary beat frequency (CBF) in human sinonasal ALI cultures. (**A**) Average traces (5-7 experiments each) showing CBF decrease in response to 1 and 10 mM denatnoium benzoate as well as inhibition of peak CBF in response to ATP after denatonium stimulation. (**B**) Denatonium benzoate-induced CBF decrease was not inhibited by the presence of 2 mM sucralose. (**C**) Denatonium-benzoate-induced CBF decrease was mimicked by application of 10 mM NaBenzoate (n = 5). This result suggests that permeation of the benzoic acid moiety may underlie the decrease in CBF. Decreased intracellular pH (acidification) has previously been shown to cause a decrease in CBF (8). (**D**) In the presence of 25 mM HCO_3^-/5% CO_2, which significantly increases intracellular H^+ buffering capacity in airway cells(9), the denatonium benzoate still induced a drop in CBF, though it was slightly blunted. Nonetheless, no increase was observed (n = 5). (**E**) The presence of the T1R agonist sucralose (2 mM) had no effect on baseline CBF (n = 5-11). No significant difference determined by Student's *t*-test. (**F**) To determine if denatonium benzoate was indeed decreasing intracellular pH, we imaged pH using the ratiometric indicator SNARF-5F. SNARF was excited at 520 nM and emission was measured using 640 and 580 nM filters as previously described (9, 10). Calibration was performed using nigericin and high [K^+] solutions of known pH as previously described (9). SNARF 640/580 emission ratio linearly reflected intracellular pH within a physiological range. (**G**) Application of denatonium benzoate caused a dose-dependent decrease in intracellular pH (mean ± SEM from 3-4 experiments each). (**H**) The decrease in intracellular pH was not affected by the presence of 5 mM glucose (mean ± SEM from 4 experiments). (**I**) Application of 10 mM NaBenzoate likewise caused a decrease in intracellular pH (mean ± SEM from 4 experiments). These data suggest that denatonium benzoate slows down CBF due to an intracellular pH decrease caused by permeation of the benzoic acid moiety. (**J** and **K**) Denatonium saccharide, absinthin amarogentin, and parthenolide failed to stimulate a significant increase in CBF (mean ± SEM from 3-6 experiments), supporting the results from **Supplemental Figure 4** suggesting that ciliated epithelial cells do not express denatonium-responsive T2Rs. Taken together, these data suggest that another sinonasal cell type mediates the observed response to denatonium and absinthin, likely solitary chemosensory cells (SCCs). In contrast, the T2R38 agonist sodium thiocyanate (NaSCN; 5 mM) caused an increase in CBF in T2R38 PAV/PAV cultures (mean ± SEM from 5 cultures from 2 patients), confirming previous results (11) that T2R38 is expressed in sinonasal ciliated epithelial cells and that its activation increases CBF.

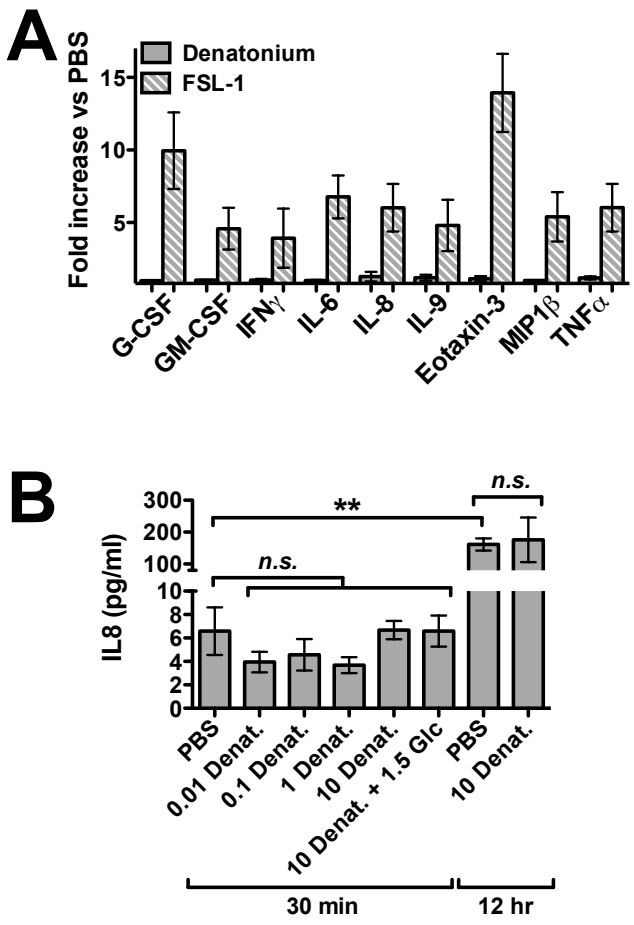

Supplemental Figure 13
Denatonium stimulation does not activate cytokine secretion. (**A**) Representative results from luminex assay showing no increase in cytokine secretion in response to 10 mM denatonium stimulation over the course of 14 hrs. Basolateral media was assayed as previously described (11). Denatonium did not stimulate an increase in any cytokine measured (n = 4 cultures from 4 patients for FSL-1 and 7 cultures from 7 patients for denatonium). Bar graph only shows cytokines for which the positive control (FSL-1) stimulated an increase in secretion. (**B**) Results were confirmed by an ELISA measure IL8 secretion. Samples of basolateral media under various conditions were assayed after 30 min and after 12 hrs. Denatonium had no effect on IL8 secretion (n = 3-8 cultures from at least 3 patients for each condition). Significance determined by 1-way ANOVA with Bonferroni post-test; ** = P <0.01, *n.s.* = no statistical significance.

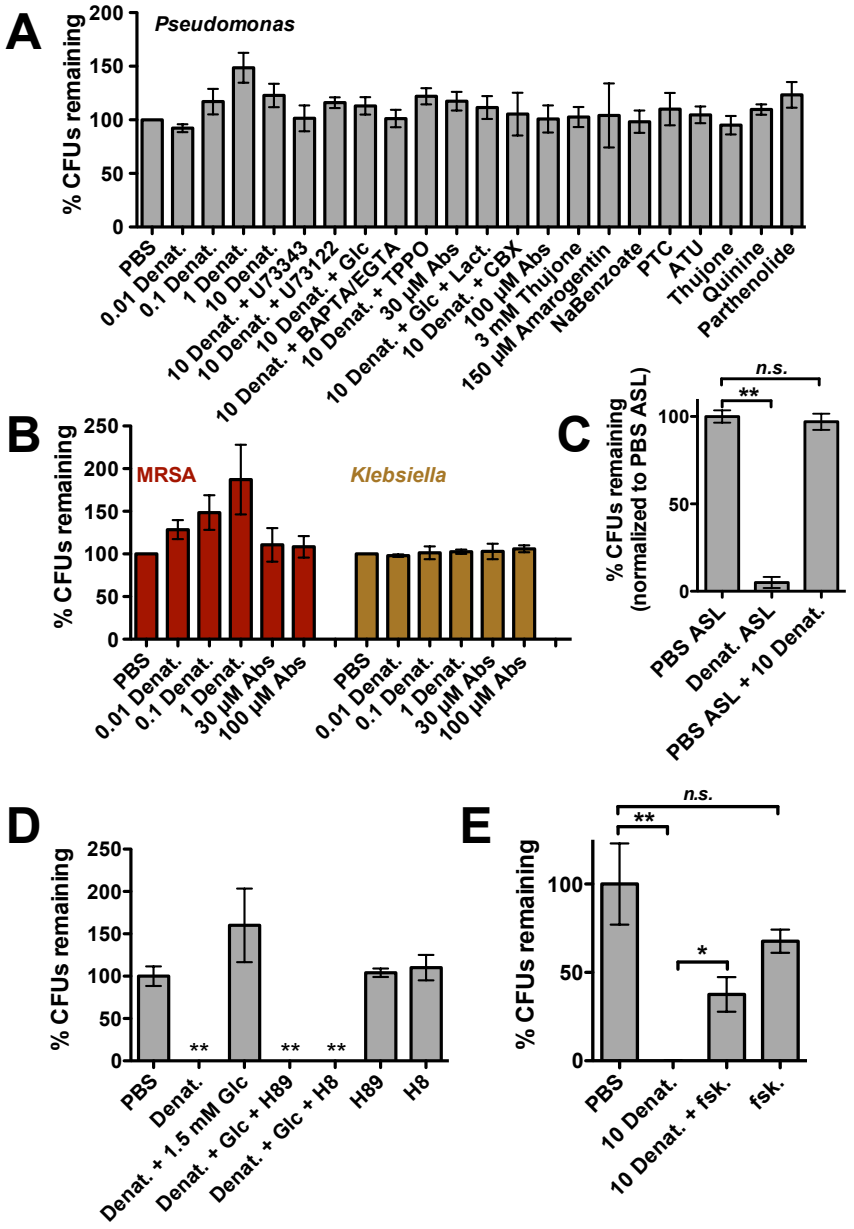

Supplemental Figure 14

Supplemental data related to bacterial kill assays. (**A-B**) Solutions used in bacterial kill assays showed no cell-independent inhibition of bacterial growth (n.s. by 1-way ANOVA). Solutions were assayed against Pseudomonas (A**;** n = 5-20 experiments) as well as MRSA and *Kebsiella* (B**;** n = 5 experiments). (**C**) Denatonium had no effects when added to PBS ASL after removal from the ALI cultures (n = 3 experiments), suggesting that bactericidal effects are due to denatonium stimulation of the ALI cultures and not synergy of denatonium with baseline secretions. Significance determined by 1-way ANOVA with Dunnett's post-test. (**D**,**E**) Inhibition of denatonium-stimulated antimicrobial secretion by glucose involves cAMP and protein kinase signaling. Glucose repression of antimicrobial secretion was blocked in the presence of the PKA/PKG inhibitors H89 and H8 (10 μM each; 10 min pre-treatment). H89 and H8 had no effects when used alone. Shown are % *Pseudomonas* CFUs remaining The response to 10 mM denatonium was inhibited by 5 min pretreatment with 10 μM forskolin. In **D**, asterisks represent significance vs PBS control determined by 1-way ANOVA with Dunnett's post test; n = 5 each; in **E**, asterisks indicate significance vs indicated groups determined by 1-way ANOVA with Tukey-Kramer post test; n = 6 each. All graphs show % *Pseudomonas* CFUs remaining; **P* <0.05; **, *P* <0.01.

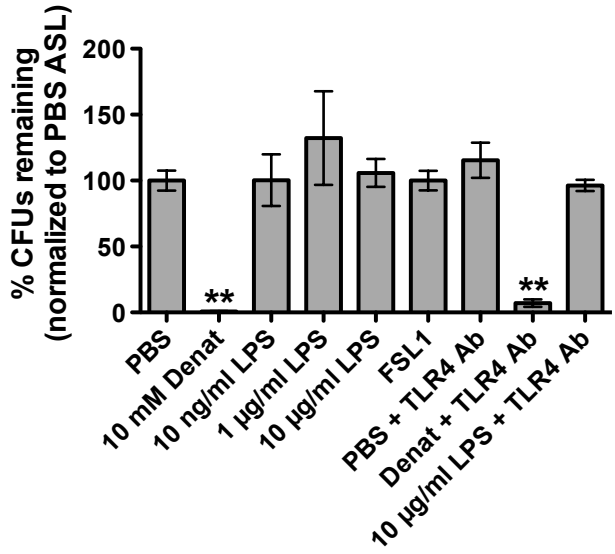

Supplemental Figure 15
Toll-like receptor (TLR) agonists (lipopolysaccharides [LPS] and FSL-1) did not stimulate acute antimicrobial peptide secretion. ASL from cultures stimulated with TLR agonists had no effect on *Pseudomonas* CFUs remaining, while denatonium-evoked antimicrobial secretion is independent of TLRs as it was not blocked by a TLR antagonist (n = 3-5 experiments each). Asterisks denote significance vs PBS (control) determined by 1-way ANOVA with Dunnett's post test. Also, no significant difference was determined between denatonium and denatonium + TLR4 Ab via 1-way ANOVA with Bonferroni post-test.

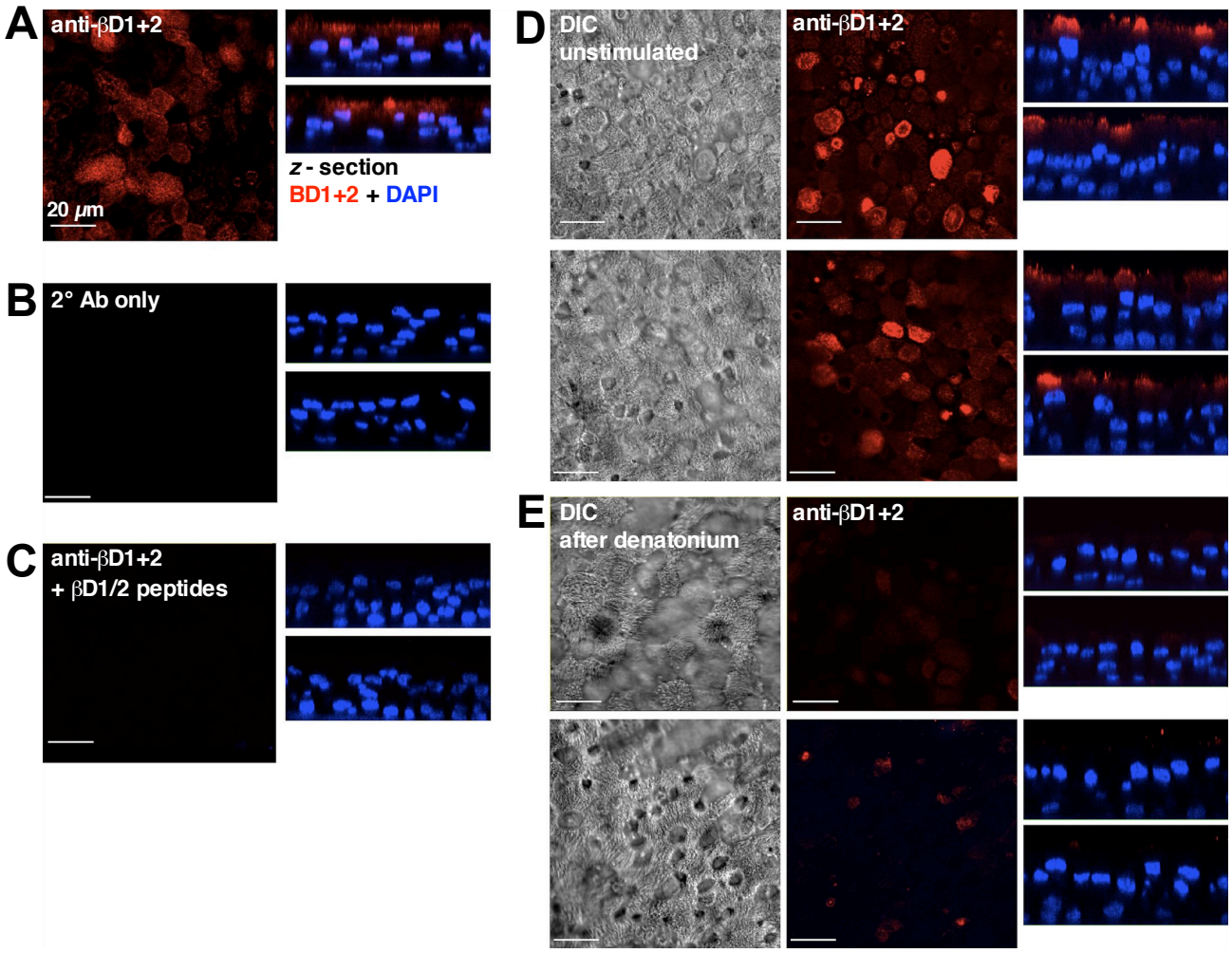

Supplemental Figure 16

Human sinonasal ALI cultures exhibite apical β-defensin immunofluorescence that is reduced after denatonium stimulation. (**A**) Human sinonasal ALI cultures were fixed with 4% formaldehyde, followed by blocking and permeabilization with 2% normal goat serum, 1% BSA, and 0.2% saponin. Primary antibodies used were rabbit polyclonal antibodies directed against human β-defensins 1 and 2 (βD1+2; shown in red) used at 1 μg/ml. Secondary antibody used was Alexafluor 549-labeled goat anti-rabbit (1:1000). Representative Z-sections show apical/mucosal side on top of the image with DAPI (a nuclear stain) in blue. β-defensin immunofluorescence was observed in the majority of cells. (**B**) No immunofluorescence was observed with secondary antibody (2° Ab) alone. (**C**) Immunofluorescence was also absent when anti-β-defensin primary antibodies were preincubated for 1 hr in the presence of recombinant β-defensins 1 and 2 (Peprotech; Rocky Hill, NJ USA) at 10 μg/ml. (**D**) Unstimulated ALIs exhibited apical fluorescence that appeared to be localized to both ciliated and nonciliated cells. (**E**) After stimulation with 10 mM denatonium for 30 min, the fluorescence signal for β-defensins was markedly reduced in the majority of cells. DIC and fluorescence images shown in (**D** and **E**) are not on the same *Z*-plane. DIC images were selected to show cilia. Fluorescence X-Y image was selected based on the slice with maximal red fluorescence, which in all cases was below (ie, more basolateral to) the level of the cilia shown in the DIC image. Cross-sections show DAPI in blue. All images shown are representative of results from 4-5 separate patients. Scale bar in all images is 20 μm.

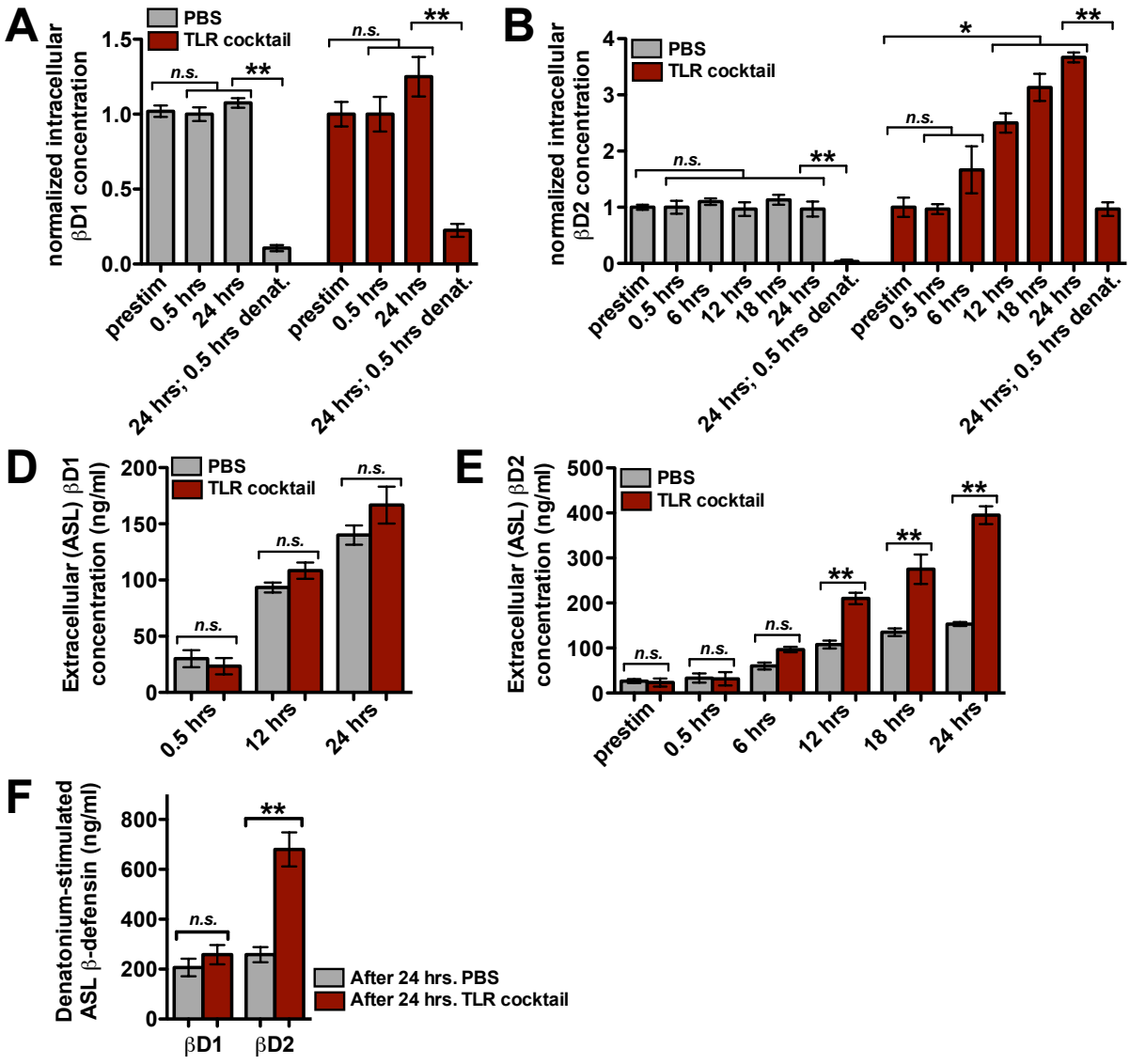

Supplemental Figure 17
Distinctions between TLR and T2R-evoked antimicrobial secretion pathways in human sinonasal epithelial cells. (**A-B**). A TLR agonist cocktail (10 µg/ml LPS, 10 µg/ml LTA, and 1 µg/ml FSL-1) stimulated an increase in intracellular β-defensin 2 (C) but not β-defensin 1 content after 12-24 hrs exposure. Stimulation with 10 mM denatonium (30 min) after 24 hrs exposure caused a release in the majority of intracellular content of both β-defensins 1 and 2. (**C-D**). TLR agonists activated an increase in extracellular β-defensin 2 (compared with PBS alone) but not β-defensin 1 at 12-24 hrs exposure. (**E**). 24 hrs exposure to a TLR agonist cocktail caused an increase in the denatonium-stimulated ASL content of β-defensin 2 but not β-defensin 1. Together, these data suggest that T2R signaling controls rapid antimicrobial release while TLR signaling controls slower but sustained antimicrobial production and release, suggesting that these are complementary pathways. Significances in B-F were determined by 1-way ANOVA with Bonferroni's post-test. For all graphs, * = P <0.05, ** = P <0.01, and *n.s.* = no statistical significance.

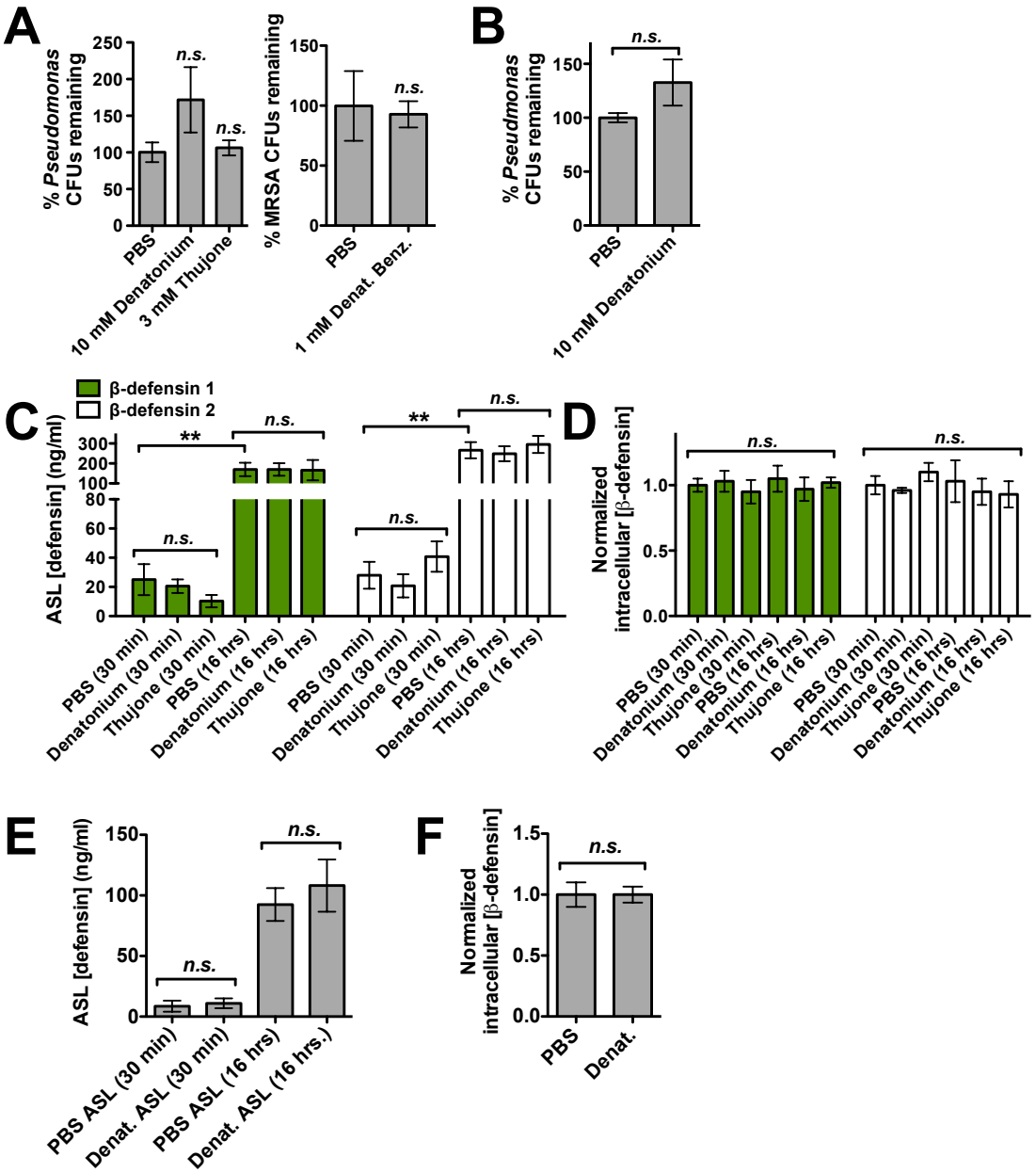

Supplemental Figure 18

T2R-activated antimicrobial peptide secretion is unique to the human upper airway. (**A**) Bacterial killing assays were performed using human bronchial epithelial (HBE) cultures. No *Pseudomonas* or MRSA killing was observed when cultures were stimulated with denatonium benzoate or thujone (no significant difference by 1-way ANOVA). These data fit with a model in which the denatonium-responsive T2Rs in the lower airway are primarily responsible for increasing CBF while the denatonium-responsive T2Rs in the upper airway are primarily responsible for activating antimicrobial peptide secretion. Bar graphs show mean ± SEM of results from 5-7 cultures from at least 3 patients each. (**B**) Bacterial killing assays were also performed with cultures derived from mouse nasal septum. Despite calcium responses to denatonium that were inhibited by glucose similarly to human sinonasal cultures (**Supplemental Figure 5**), mouse cultures did not exhibit bacterial killing (no significant difference by Student's t-test). These data suggest that the antibacterial response observed here is unique to the human upper airway. Bar graph shows mean ± SEM of 6 cultures from at least 3 different mice each. (**C**) HBE cultures did not exhibit increased secretion of β-defensins 1 (green bars) or 2 (white bars) in response to 10 mM denatonium or 3 mM thujone over the course of 30 min or 16 hrs. Asterisks denote significance as determined by 1-way ANOVA with Tukey-Kramer post-test. (**D**) HBE cultures likewise did not exhibit a decrease in intracellular β-defensin content during stimulation with denatonium. No significant differences determined by 1-way ANOVA. (**E**) Mouse nasal septal cultures likewise did not exhibit increased β-defensin secretion or a decrease in intracellular β-defensin content after stimulation with 10 mM denatonium. For all figures, * = P <0.05, ** = P <0.01, and *n.s.* = no statistical significance.

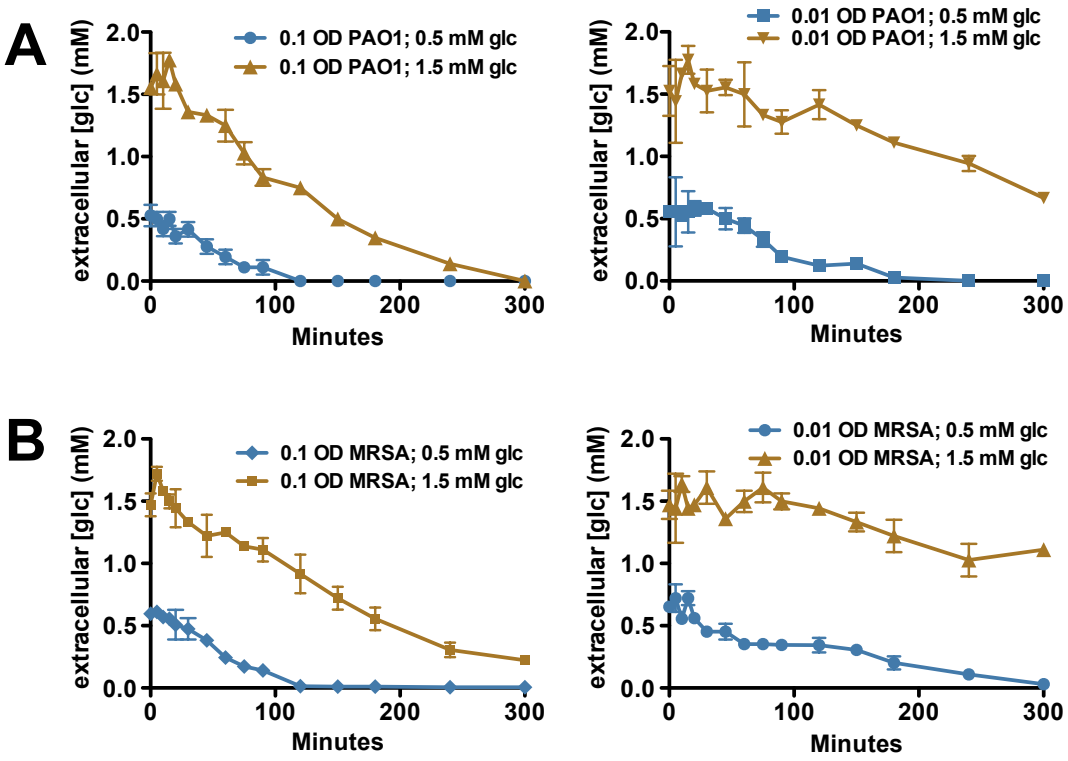

Supplemental Figure 19
Bacteria rapidly decrease the glucose concentration of ASL-like fluid. (**A-B**) *Pseudomonas aeruginosa* (strain PAO1; A) or methicillin-resistant *Staphylococcus aureus* (MRSA; B) were grown over night in LB medium, then diluted to an OD of 0.1 in LB and grown for another hour. Bacteria were then resuspended at the indicated ODs (0.1 or 0.01) in an ASL-like saline buffer (DPBS, pH 6.8) in the presence of 0.5 mM or 1.5 mM glucose. Bacteria were grown at 37 °C and samples were taken at the indicated time points. Both strains of bacteria reduced the glucose concentration at all conditions tested; glucose was depleted markedly faster when bacteria were grown in 0.5 mM glucose vs 1.5 mM glucose.

Supplemental References

1. Palmer, R.K., Atwal, K., Bakaj, I., Carlucci-Derbyshire, S., Buber, M.T., Cerne, R., Cortes, R.Y., Devantier, H.R., Jorgensen, V., Pawlyk, A., et al. 2010. Triphenylphosphine oxide is a potent and selective inhibitor of the transient receptor potential melastatin-5 ion channel. *Assay Drug Dev Technol* 8:703-713.
2. Kaske, S., Krasteva, G., Konig, P., Kummer, W., Hofmann, T., Gudermann, T., and Chubanov, V. 2007. TRPM5, a taste-signaling transient receptor potential ion-channel, is a ubiquitous signaling component in chemosensory cells. *BMC Neurosci* 8:49.
3. Meyerhof, W., Batram, C., Kuhn, C., Brockhoff, A., Chudoba, E., Bufe, B., Appendino, G., and Behrens, M. 2010. The molecular receptive ranges of human TAS2R bitter taste receptors. *Chem Senses* 35:157-170.
4. Wiener, A., Shudler, M., Levit, A., and Niv, M.Y. 2012. BitterDB: a database of bitter compounds. *Nucleic Acids Res* 40:D413-419.
5. Damak, S., Rong, M., Yasumatsu, K., Kokrashvili, Z., Varadarajan, V., Zou, S., Jiang, P., Ninomiya, Y., and Margolskee, R.F. 2003. Detection of sweet and umami taste in the absence of taste receptor T1r3. *Science* 301:850-853.
6. Damak, S., Rong, M., Yasumatsu, K., Kokrashvili, Z., Perez, C.A., Shigemura, N., Yoshida, R., Mosinger, B., Jr., Glendinning, J.I., Ninomiya, Y., et al. 2006. Trpm5 null mice respond to bitter, sweet, and umami compounds. *Chem Senses* 31:253-264.
7. Wong, G.T., Gannon, K.S., and Margolskee, R.F. 1996. Transduction of bitter and sweet taste by gustducin. *Nature* 381:796-800.
8. Sutto, Z., Conner, G.E., and Salathe, M. 2004. Regulation of human airway ciliary beat frequency by intracellular pH. *J Physiol* 560:519-532.
9. Lee, R.J., Harlow, J.M., Limberis, M.P., Wilson, J.M., and Foskett, J.K. 2008. HCO3(-) secretion by murine nasal submucosal gland serous acinar cells during Ca^{2+}-stimulated fluid secretion. *J Gen Physiol* 132:161-183.
10. Kreindler, J.L., Bertrand, C.A., Lee, R.J., Karasic, T., Aujla, S., Pilewski, J.M., Frizzell, R.A., and Kolls, J.K. 2009. Interleukin-17A induces bicarbonate secretion in normal human bronchial epithelial cells. *Am J Physiol Lung Cell Mol Physiol* 296:L257-266.
11. Lee, R.J., Xiong, G., Kofonow, J.M., Chen, B., Lysenko, A., Jiang, P., Abraham, V., Doghramji, L., Adappa, N.D., Palmer, J.N., et al. 2012. T2R38 taste receptor polymorphisms underlie susceptibility to upper respiratory infection. *J Clin Invest* 122:4145-4159.